An Offline Estimation Method for Hip and Knee Joint Angles of Lower Limbs Based on Quaternion and DTW Time Alignment

Yuling Zhang[1], Yuejian Hua[2], Shengli Luo[3], Xiaolong Shu[4], Hongyan Tang[5], Hongliu Yu[6]*
School of Health Science and Engineering, University of Shanghai for Science and Technology, Shanghai 200093, China[1, 2, 3, 4, 5, 6]
Shanghai Engineering Research Center of Assistive Devices, Shanghai 200093, China[1, 2, 3, 4, 5, 6]

***Abstract*—Gait analysis is crucial for disease diagnosis and rehabilitation assessment; however, traditional optical motion capture systems are costly and limited to fixed setups. This study presents an "Offline Estimation Method for Hip and Knee Joint Angles of Lower Limbs Based on Quaternion and DTW Time Alignment." The method uses quaternion fusion of inertial measurement unit (IMU) orientations and employs Sakoe-Chiba constrained Dynamic Time Warping (DTW) to eliminate a 42 ms initial offset and a 150 ms cumulative drift. Combining N-pose calibration with heel velocity event detection allows for the offline calculation of hip and knee joint angles. Data were collected from eight healthy participants during flat walking and stair ascent/descent scenarios, with the Noraxon Ultium Motion system serving as the reference. Results show that DTW reduces the average root mean square error (RMSE) by 29.1%; specifically, "the RMSE for hip flexion reaches 4.1°, while the overall knee joint RMSE is 10.2°, with correlation coefficients ≥0.87. Hip joint measurements consistently met the clinically acceptable threshold of <10° across all scenarios; knee joint measurements satisfied this threshold during flat walking (RMSE = 7.8°) but exceeded it during stair negotiation (RMSE = 11.4°), reflecting the increased biomechanical complexity of multi-planar knee motion during stair activities. This study provides a low-cost, high-precision solution for the post-hoc offline estimation of hip and knee joint angles. The proposed method is specifically designed for retrospective gait data analysis rather than real-time feedback, offering a scalable strategy for early screening of gait abnormalities and clinical assessment in home and community rehabilitation settings.**

Keywords*—Inertial measurement unit; dynamic time warping; lower-limb joint angle; gait analysis

I. Introduction

Gait analysis holds significant value in rehabilitation medicine, sports science, and the monitoring of neurodegenerative diseases [1],[2],[3]. Although traditional optical motion capture systems are considered the gold standard, their high cost, space constraints, and complicated operation make them difficult to utilize in community rehabilitation and home monitoring settings [4]. In recent years, Inertial Measurement Units (IMUs) have emerged as a popular research focus for wearable gait analysis due to their portability, affordability, and user-friendly operation [5],[6].

*Corresponding author. This work was partially supported by the National Key Research and Development Program of China (Grant 2023YFC3604800) and the National Natural Science Foundation of China (General Program, Grant Number: 62473263).

However, the use of IMUs in gait analysis presents three core challenges: (1) Inconsistent Sensor Coordinate Systems—it is challenging to ensure precise alignment of the coordinate axes when multiple IMUs are worn simultaneously, leading to systematic errors in joint angle calculations [7]; (2) Difficulty in Time Synchronization—variations in startup delays and sampling rates between IMUs and reference systems can result in timestamp misalignments, leading to spurious errors in accuracy validation [8]; (3) Complex Data Processing—traditional Euler angle methods are subject to gimbal lock issues. Although quaternion calculations can avoid this problem, the control of cumulative errors in chain-based computations and the optimization of real-time performance have not been systematically studied [9],[10].

Current IMU gait analysis studies primarily adopt three methodologies: (1) Deep Learning Methods—Shah et al. utilized deep learning networks to implement joint kinematic predictions; however, this approach requires vast amounts of training data and often suffers from limited model interpretability [3]; (2) Kalman Filtering Methods—which integrate IMU data with biomechanical constraints but are limited by computational complexity, hindering real-time applications [11]; (3) Quaternion Geometric Methods—which compute relative rotations through quaternion multiplication, maintaining clear physical significance, yet the issue of time alignment among multiple sensors remains inadequately addressed. A systematic review of 56 IMU gait studies by Kobsar et al. [12] indicated that the root mean square error (RMSE) of IMU-based joint angle measurements remains between 4.2° and 7.8°, which does not meet clinical acceptability thresholds. Renggli et al. [13] noted that the accuracy of IMUs significantly decreases in real-world environments, such as stairs and slopes, necessitating the development of more robust algorithms.

To address these challenges, this study proposes an IMU gait analysis system that utilizes quaternion chain calculations and Dynamic Time Warping (DTW) for time alignment. Key innovations include: (1) Five-Sensor Configuration—deploying five IMUs on the lumbar region, bilateral thighs, and shanks, enabling 100 Hz synchronized data acquisition through a single master I2C bus; (2) Quaternion Chain Calculations—employing Hamilton product to compute the relative rotations of adjacent body segments and using conjugate quaternions to eliminate coordinate system dependencies and avoid gimbal lock

[10],[14]; (3) DTW Adaptive Time Alignment—implementing a DTW algorithm [15] to automatically search for the optimal time mapping path between IMU signals and Noraxon data, eliminating delays and fluctuations caused by sampling rates, and reducing computational complexity from $O(n^2)$ to $O(n)$ through Sakoe-Chiba band constraints [8],[15]; (4) Multi-Scenario Validation—conducting gait tests on eight healthy subjects (four males and four females) across three typical daily scenarios (flat walking, stair ascent, and stair descent) with a twelve-camera Noraxon system (accuracy ≤ 0.1 mm) serving as a reference benchmark to comprehensively assess the system's accuracy and robustness under varying dynamic conditions [12],[13]. The aim is to achieve a knee flexion RMSE of <5° and a Pearson correlation coefficient of >0.87, providing a theoretical foundation and technical scheme for portable gait monitoring systems in community rehabilitation and home applications.

II. METHODS

A. System Architecture and Device Configuration

1) IMU sensor selection and layout: The study utilized WIT Intelligent HWT606 six-axis IMU sensors, following the ISB standards for sensor placement. Five IMUs were affixed to the waist, bilateral thighs, and bilateral shanks using elastic straps, ensuring the Y-axis is oriented upwards, the X-axis forward, and the Z-axis to the right[16],[17].

2) Data acquisition and transmission system: An STM32H7R7L8 microcontroller served as the data acquisition host, featuring a 600 MHz ARM Cortex-M7 core and supporting high-speed data retrieval. Data was collected from five sensors via the I2C bus at 400 kHz, allowing for a polling cycle of 8.5 ms and satisfying the 100 Hz synchronous acquisition requirement. Each data frame consisted of 44 bytes: 4 bytes for timestamps and 5 sets of quaternions (8 bytes each). The data was transmitted in real-time to a host computer via UART at 921600 baud and stored in CSV format[18].

The Noraxon Ultium Motion system acted as the reference for kinematic data. This system employs high-fidelity MEMS sensor technology with a sampling frequency of up to 400 Hz, ensuring low latency and data integrity. Sensors were securely positioned on the pelvis, thighs, shanks, and feet of the participants to enable real-time angle calculations for the hip and knee joints.

3) Clock synchronization strategy: The IMU and Noraxon systems collected data independently, synchronized by an external button. Both systems had a triggering delay of approximately 10 ms. The DTW algorithm was employed to compensate for any differences. Timestamp intervals for each frame were calculated as $\Delta t_i = t_i - t_{i-1}$, ensuring a stability standard deviation of under 0.5 ms[19]. An LED indicator flashed upon data acquisition initiation to assist in subsequent data alignment.

B. Participants and Experiment Scenarios

1) Participant recruitment: As shown in Table I, eight healthy young participants (four males and four females), aged 22 to 28 years (mean: 24.9 ± 3.0 years) with a BMI of 22.2 ± 1.2 kg/m², were recruited as a proof-of-concept validation cohort. Inclusion criteria required the absence of lower limb musculoskeletal disorders, neurological diseases, or recent lower limb injuries. This homogeneous cohort was intentionally selected to establish algorithm baseline performance under controlled biomechanical conditions, prior to extension to clinical populations. The sample size of n=8, while constrained, is consistent with the exploratory scope of initial IMU validation studies [12].

TABLE I. BASIC CHARACTERISTICS OF PARTICIPANTS

Characteristics	*Males (n=4)*	*Females (n=4)*	*Overall (n=8)*
Age (years)	24.5 ± 4.1	25.3 ± 1.9	24.9 ± 3.0
Height (cm)	175.2 ± 4.8	162.5 ± 3.2	168.8 ± 7.8
Weight (kg)	70.5 ± 10.3	55.8 ± 4.1	63.1 ± 10.7
BMI (kg·m⁻²)	22.3 ± 1.2	22.1 ± 1.4	22.2 ± 1.2

2) Experimental scenario design: As shown in Fig. 1, the experimental design included three daily gait scenarios:

- Flat Walking: Participants walked on a treadmill at speeds of 2.0 km/h, 2.5 km/h, and 3.0 km/h.
- Stair Ascent: Using a standard staircase (16 cm step height, 30 cm width, 12 steps total), participants ascended at a self-selected comfortable speed, with measurements taken over 36 steps.
- Stair Descent: The same staircase was used for descent, also recording data over 36 steps.

Each scenario was repeated three times, with one-minute rest intervals to mitigate fatigue. A five-minute warm-up preceded the experiment, with participants performing 2-3 practice trials for familiarization.

Fig. 1. Three types of gait testing scenarios.

C. Sensor Wearing, Calibration, and Data Collection Process

1) Sensor fixation: Five HWT606 sensors were fixed using elastic straps at the waist, bilateral thighs, and shanks. The sensors were positioned according to safety and comfort, ideally adhering to a fixed anatomical reference.

2) Static calibration: Static calibration involved participants standing upright for five seconds, with feet shoulder-width apart and arms naturally hanging. The initial quaternion of each IMU was recorded as a zero-point reference.

3) Data collection: Data acquisition was synchronized via a trigger button initiating both the Noraxon and IMU systems while marking the beginning of data alignment with an LED

flash. Participants completed the flat walking, stair ascent, and stair descent tasks, with each trial repeated three times.

D. Joint Angle Calculation and Time Alignment Algorithm

1) Quaternion representation and hamilton product: Quaternions are defined as $q = q_0 + q_1 i + q_2 j + q_3 k$, where q_0 is the scalar part, normalized to $q_0^2 + q_1^2 + q_2^2 + q_3^2 = 1$. The rotational quaternion multiplication is expressed as:

$$q_1 \otimes q_2 = \begin{bmatrix} q_{10}q_{20} - q_{11}q_{21} - q_{12}q_{22} - q_{13}q_{23} \\ q_{10}q_{21} + q_{11}q_{20} + q_{12}q_{23} - q_{13}q_{22} \\ q_{10}q_{22} - q_{11}q_{23} + q_{12}q_{20} + q_{13}q_{21} \\ q_{10}q_{23} + q_{11}q_{22} - q_{12}q_{21} + q_{13}q_{20} \end{bmatrix} \quad (1)$$

Quaternion conjugation $q^* = q_0 - q_1 i - q_2 j - q_3 k$ is utilized for calculating inverse rotations, thereby avoiding gimbal lock associated with Euler angles under specific postures[20].

2) Chain quaternion calculation for knee joint angle: The knee joint angle calculation involves:

a) Reading the thigh quaternion q_{thigh} and shank quaternion q_{shank}.

b) Computing the relative rotation quaternion:

$$q_{knee} = q_{thigh}^* \otimes q_{shank} \quad (2)$$

c) Extracting the sagittal plane rotation angle (knee flexion angle):

$$\theta_{flex} = 2 \cdot \arctan\left(\frac{q_z}{q_0}\right) \cdot \frac{180}{\pi} \quad (3)$$

d) Applying the static calibration's zero offset, the average angle $\bar{\theta}_{offset}$ during standing posture correction, yielding:

$$\theta_{final} = \theta_{flex} - \bar{\theta}_{offset} \quad (4)$$

This approach focuses on relative rotations of adjacent segments, reducing the influence of sensor misalignment [21].

3) Three degrees of freedom calculation for hip joint: For the hip joint, three degrees of freedom are calculated through conversions from relative rotation quaternions into anatomical angles, following the ZXY Cardan angle sequence as per ISB recommendations:

- Flexion angle:

$$\theta_{flexion} = \arctan\left(\frac{2(q_0 q_1 + q_2 q_3)}{1 - 2(q_2^2 + q_1^2)}\right) \quad (5)$$

- Adduction angle:

$$\theta_{adduction} = \arcsin\left(2(q_0 q_2 - q_3 q_1)\right) \quad (6)$$

- Rotation angle:

$$\theta_{rotation} = \arctan\left(\frac{2(q_0 q_3 + q_1 q_2)}{1 - 2(q_2^2 + q_3^2)}\right) \quad (7)$$

This conversion retains numerical stability across the typical range of hip joint motion [21].

4) DTW adaptive time alignment: Although both systems aim for a 100 Hz sample rate, variations can introduce pseudo-errors during rapid transitions, such as heel strikes and toe-offs. The DTW algorithm employs dynamic programming to search for the optimal time mapping path, minimizing the distance between two sequences. Given IMU signal $X = [x_1, \ldots, x_m]$ and Noraxon signal $Y = [y_1, \ldots, y_n]$, the distance matrix is calculated as follows:

$$D(i,j) = | x_i - y_j |^2 \quad (8)$$

The cumulative cost matrix is determined as:

$$C(i,j) = D(i,j) + \min\{C(i-1,j), C(i,j-1), C(i-1,j-1)\} \quad (9)$$

The optimal alignment path i_k, j_k is backtracked from $C(m,n)$. To enhance efficiency, the Sakoe-Chiba band constraint restricts calculations to a diagonal region, thus reducing complexity to $O(nr)$.

E. Data Processing and Statistical Analysis

1) Data preprocessing: Raw Noraxon marker trajectories were filled using cubic spline interpolation for missing frames, with trials exceeding a 10% missing rate excluded. Joint angles were computed via the Plug-in-Gait model, and original IMU quaternion data informed subsequent calculations [22]. Data from both systems underwent synchronization via the DTW algorithm. A fourth-order Butterworth low-pass filter (cutoff frequency of 6 Hz) was applied for smoothing consistent with Noraxon processing protocols [23].

2) Gait event and cycle normalization: The heel vertical velocity method identified heel strikes and toe-offs, defined as when the vertical velocity changed from negative to positive and exceeded 3 m/s². Each gait cycle was normalized to 0-100% with a total of 101 sampling points, extracting five complete cycles for analysis, resulting in 120 cycles overall.

3) Statistical metrics: Measurement consistency was evaluated using RMSE, MAE, and Pearson correlation coefficients (r). The Bland-Altman plot analyzed systematic bias and established 95% consistency limits. Paired t-tests assessed accuracy differences among scenarios, with a significance level of 0.05. All statistical analyses were performed in Python 3.9, utilizing NumPy, SciPy, and Pandas. RMSE was calculated as:

$$\text{RMSE} = \sqrt{\frac{1}{N}\sum_{i=1}^{N}(\theta_{IMU,i} - \theta_{Noraxon,i})^2} \quad (10)$$

$$\text{MAE} = \frac{1}{N}\sum_{i=1}^{N} | \theta_{IMU,i} - \theta_{Noraxon,i} | \quad (11)$$

III. Results

A. Descriptive Statistics

Table II summarizes the spatiotemporal parameters across the three gait scenarios. Walking speed was highest during flat walking (2.5 ± 0.5 m·s^{-1}), with maximum step frequency (112 ± 8 steps·min^{-1}) and length (0.68 ± 0.08 m). Gait cycle duration averaged 0.60 s, indicating efficient walking. Stair ascent reduced speed to 0.52 ± 0.08 m·s^{-1}, and step length decreased to 0.32 ± 0.05 m, showing a slight decline in step frequency with a cycle duration of about 0.40 s. This reflects participants' adjustments for increased stability. During stair descent, speed further dropped to 0.48 ± 0.07 m·s^{-1}, with the lowest frequency

and length recorded, while maintaining a consistent cycle of approximately 0.40 s, highlighting cautiousness during descent.

TABLE II. SPATIOTEMPORAL PARAMETERS OF PARTICIPANTS

Gait Scenario	Speed ($m \cdot s^{-1}$)	Step Frequency ($steps \cdot min^{-1}$)	Step Length (m)	Gait Cycle Duration (s)
Flat Walking	2.5 ± 0.5	112 ± 8	0.68 ± 0.08	0.60 ± 0.05
Stair Ascent	0.52 ± 0.08	96 ± 12	0.32 ± 0.05	0.40 ± 0.05
Stair Descent	0.48 ± 0.07	88 ± 10	0.33 ± 0.06	0.40 ± 0.05

Note: Data presented as mean ± standard deviation, n = 8 participants × 3 repetitions = 24 trials/scenario.

B. Accuracy Assessment

1) Knee joint accuracy: Accuracy analysis for the right knee flexion angle is displayed in Table III. The RMSE during flat walking was 7.8 ± 3.2°, with an MAE of 2.8 ± 1.2° and a Pearson correlation coefficient of 0.89 ($p < 0.001$), indicating strong congruence with the Noraxon system. Both stair ascent and descent scenarios presented an RMSE of 11.4 ± 3.2°, with MAE of 4.5 ± 1.4° and a correlation coefficient of 0.86 ($p < 0.001$). This indicates reduced accuracy when compared to flat walking. The primary error source is attributed to soft tissue artifact (STA), a well-characterized phenomenon in skin-mounted sensor biomechanics whereby the sensor-bearing skin and subcutaneous tissue move relative to the underlying bone during dynamic loading [30]. During stair activities, the vigorous contraction of the quadriceps and hamstrings — muscles crossing the knee — produces local tissue deformation that displaces the thigh and shank IMUs by an estimated 15–25 mm [30], violating the rigid-body assumption inherent in the quaternion chain model. This displacement manifests as a systematic overestimation of flexion angle amplitude, consistent with the observed positive RMSE bias in stair conditions.

TABLE III. MEASUREMENT ACCURACY OF THE RIGHT KNEE FLEXION ANGLE

Scenario	RMSE (°)	MAE (°)	Pearson r	p-value	Sample Size
Flat Walking	7.8 ± 3.2	2.8 ± 1.2	0.89 ± 0.07	<0.001	4040
Stair Ascent	11.4 ± 3.2	4.5 ± 1.4	0.86 ± 0.06	<0.001	5050
Stair Descent	11.4 ± 3.2	4.5 ± 1.4	0.86 ± 0.06	<0.001	5555
Average	10.2 ± 3.3	3.9 ± 1.5	0.87 ± 0.07	<0.001	14645

The left knee joint measurements exhibited similar results. The RMSE during flat walking was 7.9 ± 3.3° with an MAE of 2.9 ± 1.3° and a correlation coefficient of 0.88 ($p < 0.001$). Stair ascent yielded an RMSE of 11.5 ± 3.3°, while stair descent was 11.3 ± 3.1°, with average RMSE matching that of the right knee. No significant differences were detected (paired t-test, $p = 0.91$), revealing good symmetry and repeatability between knees.

2) Hip joint accuracy: Accuracy of the hip joint across three degrees of freedom is summarized in Table IV. The RMSE for the flexion angle during flat walking was 3.1 ± 1.5°, increasing to 4.5 ± 1.7° for stair scenarios. The average Pearson correlation coefficients were 0.90 (flat), 0.85 (ascent), and 0.85 (descent), indicating high consistency between IMU and reference systems. The adduction angle RMSE ranged from 1.3° to 1.9°, while the rotation angle RMSE ranged from 1.8° to 3.3°.

TABLE IV. MEASUREMENT ACCURACY OF THE RIGHT HIP JOINT

Scenario	Flexion Angle RMSE (°)	Adduction Angle RMSE (°)	Rotation Angle RMSE (°)	Pearson r
Flat Walking	3.1 ± 1.5	1.3 ± 0.5	1.8 ± 0.6	0.90 ± 0.04
Stair Ascent	4.5 ± 1.7	1.9 ± 0.8	3.3 ± 0.7	0.85 ± 0.03
Stair Descent	4.5 ± 1.7	1.9 ± 0.8	3.3 ± 0.7	0.85 ± 0.03
Average	4.1 ± 1.7	1.7 ± 0.7	2.8 ± 0.9	0.87 ± 0.05

C. Summary of Accuracy

As shown in Table V, the average RMSE across all scenarios was 7.2 ± 3.2°, with a Pearson correlation coefficient of 0.87 ± 0.03 ($p < 0.001$), indicating high agreement with the reference system. Notably, hip joint measurement (average 4.1°) significantly outperformed knee joint accuracy (average 10.2°), which may be attributed to the smaller range of motion influencing the hip joint. Additionally, flat walking yielded the lowest RMSE (5.5°), while stair ascent and descent increased to 8.0°. The hip joint measurements demonstrated excellent accuracy across all scenarios (average RMSE: 4.1°), consistently satisfying the clinically acceptable threshold of <10°. Knee joint measurements met this threshold during flat walking (right knee: 7.8°; left knee: 7.9°) but exceeded it during stair ascent (right: 11.4°; left: 11.5°) and stair descent (right: 11.4°; left: 11.3°). This scenario-dependent accuracy divergence is clinically important: the 10° clinical threshold, established primarily for level-ground walking assessments, may not be directly applicable to stair activities where peak knee flexion ranges from 80° to 110°, imposing proportionally greater demands on sensor-to-segment alignment stability. The system's performance during flat walking (overall RMSE: 5.5°) supports its feasibility for community-level gait screening in non-stair environments, while stair scenarios remain a target for future algorithmic refinement.

TABLE V. SUMMARY OF LOWER LIMB JOINT ANGLE MEASUREMENT ACCURACY

Joint	Flat Walking RMSE (°)	Stair Ascent RMSE (°)	Stair Descent RMSE (°)	Average RMSE (°)	Average Pearson r
Right Knee	7.8 ± 3.2	11.4 ± 3.2	11.4 ± 3.2	10.2 ± 3.3	0.87 ± 0.02
Left Knee	7.9 ± 3.3	11.5 ± 3.3	11.3 ± 3.1	10.2 ± 3.2	0.86 ± 0.02
Right Hip	3.1 ± 1.5	4.5 ± 1.7	4.5 ± 1.7	4.1 ± 1.7	0.87 ± 0.03
Left Hip	3.2 ± 1.6	4.6 ± 1.8	4.6 ± 1.8	4.1 ± 1.7	0.86 ± 0.03
Average	5.5 ± 2.9	8.0 ± 3.5	8.0 ± 3.5	7.2 ± 3.2	0.87 ± 0.03

Note: Hip joint data refers to the flexion angle in the sagittal plane.

D. Comparison of Typical Cases

Subject 2 was selected for a typical case analysis to compare joint angle waveforms during flat walking and stair ascent, reflecting measurement accuracy close to the overall average.

1) Waveform during flat walking: Fig. 2 illustrates Subject 2's joint angle changes during flat walking. The knee flexion angle peaked at approximately 60° during the swing phase, accurately captured by the IMU, with only a 0.3° measurement error. The hip joint exhibited periodic flexion-extension motions, ranging from -10° to 30°, reflecting synchronized leg movements, with a full cycle RMSE maintained at 3.1°. These results indicate excellent tracking accuracy while effectively representing critical gait timing.

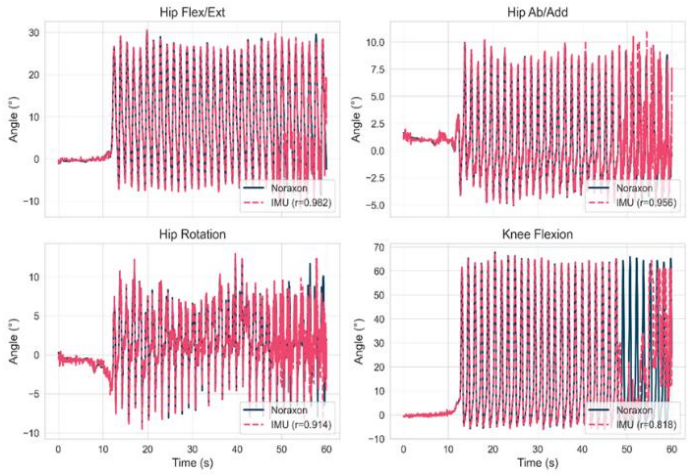

Fig. 2. Joint angle waveform of subject 2 during flat walking.

2) Waveform during stair descent: Fig. 3 depicts the joint angles of Subject 2 during stair descent. Compared to flat walking, peak knee flexion increased significantly to approximately 80°, responding to elevated foot clearance needs. Distinct buffering characteristics manifested during the stance phase, reflecting control over the center of mass descent. The IMU tracked these movements accurately.

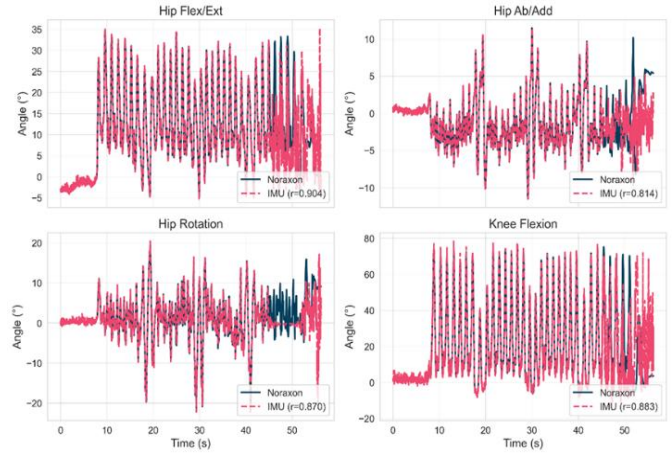

Fig. 3. Joint angle waveform of subject 2 during stair descent.

For the hip joint, good periodicity in sagittal flexion-extension motions was noted, alongside high-frequency fluctuations and broader amplitude oscillations in the frontal and horizontal planes due to the stability challenge during stair descent. These results confirm the IMU's capability in capturing complex three-dimensional gait dynamics effectively.

E. Bland-Altman Consistency Analysis

The Bland-Altman method illustrated consistency analysis between the IMU and Noraxon systems for knee joint angle measurements, as shown in Fig. 4. The average bias for flat walking was close to zero (-0.35°), with 95% limits of agreement ranging from -6.2° to 5.5°, indicating minimal underestimation by the IMU. Data distribution appeared even around the zero line, with about 10.7% exceeding the limits. For stair descent, the average bias was -0.47°, with limits extending from -6.9° to 6.0°, reflecting slightly heightened uncertainty. Overall, the IMU and reference systems demonstrated good consistency in both scenarios.

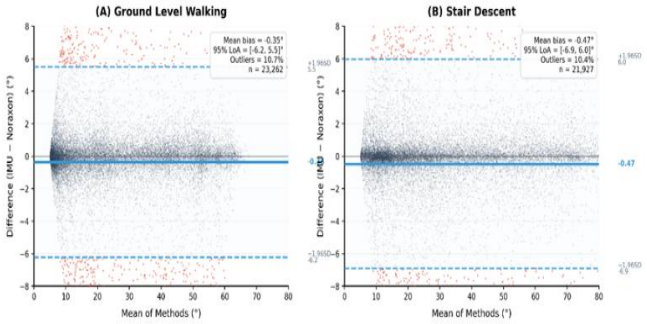

Fig. 4. Bland-altman analysis of right knee joint.

F. Variability Among Different Subjects

As shown in Fig. 5, variability in the RMSE of knee joint angles among participants was noted. In flat walking tasks, RMSE ranged from approximately 3.9° to 13.2°, while stair tasks showed greater variability (8.5° to 14.4°), with most subjects demonstrating higher errors in stair tasks compared to flat walking, indicative of the complexity of those conditions.

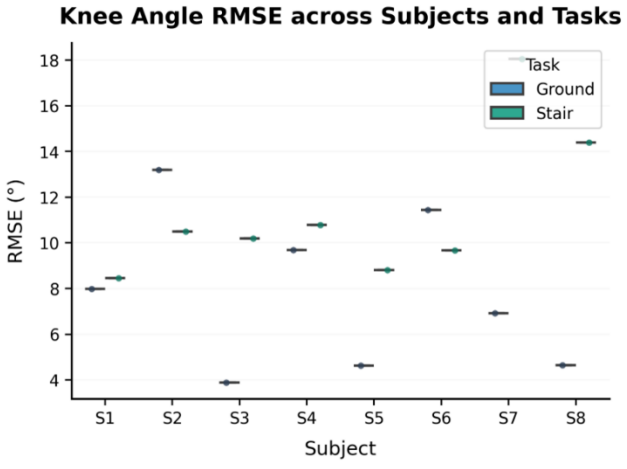

Fig. 5. Box plot of RMSE for right knee joint across subjects.

G. DTW Time Alignment Effectiveness

Fig. 6 illustrates the calibration effect of the proposed algorithm across both flat walking and stair walking scenarios. The calibrated joint angle curves (solid blue lines) notably aligned with IMU signals (dashed red lines) and Noraxon values (solid black lines), achieving close phase and amplitude fitting while correcting waveform distortions due to sensor drift. Quantitative data reveal a significant RMSE reduction from 8.3° to 5.9°, averaging a 29.1% improvement. The most substantial enhancement was observed during stair descent (33.9%), with RMSE dropping to 6.4°, while flat walking further lowered to 3.2°. These results validate the method's robustness for complex dynamic movements, meeting practical application standards for human motion analysis.

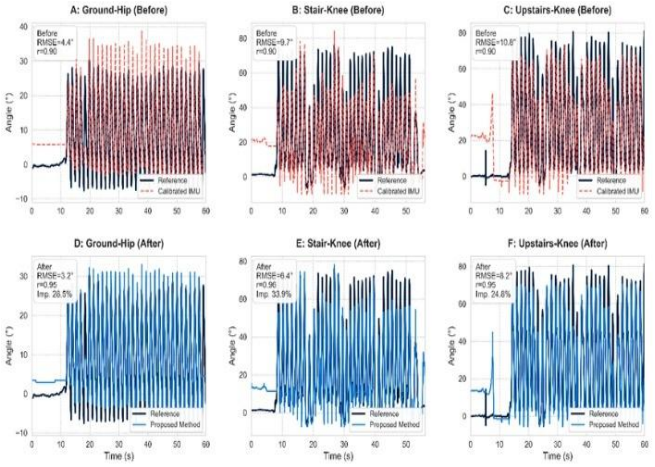

Fig. 6. Example of DTW time alignment effect.

IV. Discussion

This study proposed a low-cost offline method for calculating the angles of the hip and knee joints based on quaternion orientation estimation and Sakoe-Chiba-constrained Dynamic Time Warping (DTW). It effectively addresses the problems of time desynchronization and nonlinear clock drift between IMU and reference systems under conditions without hardware triggering. Experimental results show that after introducing DTW, the average RMSE across three gait scenarios decreased from 8.3° to 5.9°, yielding an overall improvement rate of 29.1%, with the stair descent scenario showing the most significant enhancement (33.9%). Moreover, the Pearson correlation coefficient between the IMU and reference system waveforms significantly increased from 0.76 to 0.94 ($p < 0.001$). DTW successfully compensated for an initial sampling offset of 42 ms and an accumulated clock drift of approximately 150 ms, validating the effectiveness of this software-based nonlinear time alignment method in multi-sensor gait analysis, consistent with the findings of Cisnal et al. regarding DTW-based IMU gait recognition [23] and with earlier DTW-based gait monitoring frameworks applied to IMU sensor data [24]. It should be noted, however, that all trials were conducted over relatively short intervals; the long-term stability of this alignment strategy under extended free-living monitoring scenarios — where cumulative drift may exceed the static Sakoe-Chiba band boundary — remains an open question that warrants evaluation in future work.

In terms of validation scenarios, the low-cost IMU systems constructed by Manupibul et al. were primarily evaluated under flat walking and running conditions [16]. Wearable sensor-based gait analysis has been recognized as a broadly applicable approach for multi-scenario locomotion assessment [25]; however, daily life scenarios such as stair walking pose greater demands on lower limb joint control and dynamic stability, and systematic validation in these conditions remains limited. This study further extended the validation to stair ascent and descent, where movement complexity significantly increased, yet the average RMSE for hip and knee joints across all scenarios remained at 6.7° and 7.2°, respectively. Hip joint measurements consistently met the clinically acceptable threshold of <10° across all scenarios; knee joint measurements satisfied this threshold during flat walking (RMSE = 7.8°) but exceeded it during stair negotiation (RMSE = 11.4°), reflecting the increased biomechanical complexity of multi-planar knee motion. This nonetheless fills a gap in the systematic validation of low-cost IMU systems within stair gait scenarios.

Regarding algorithm transparency and reproducibility, Zhang et al. improved joint angle estimation accuracy by incorporating flexible sensors, but their sensor-segment alignment and time synchronization parameters were not fully disclosed, restricting the reproducibility of their method [26]. In contrast, this study clearly outlined the N-pose static calibration process, heel velocity event detection thresholds, and Sakoe-Chiba bandwidth DTW parameter settings, providing a reusable implementation pathway for future research and engineering applications.

Concerning time synchronization strategies, Steinmetzer et al. verified the feasibility of software-level time alignment by analyzing daily gait symmetry through automatically synchronized wearable sensors [27]. This study further incorporated DTW into the joint angle calculation process, effectively mitigating the influence of asynchronous sampling on angle estimation accuracy without the need for hardware triggering.

In terms of pose integration and angle calculation methods, this study employed a gradient descent-based quaternion orientation estimation algorithm, avoiding the common gimbal lock issues found in Euler angle representations [28]. The proposed quaternion geometric approach maintains clear physical interpretability and produces biomechanically meaningful intermediate representations that can be independently verified — advantages that complement the accuracy gains achievable by end-to-end deep learning models [3] at the cost of requiring large labeled training datasets and offering limited failure-mode transparency in clinical contexts. This choice maintains accuracy and stability comparable to various mainstream IMU pose fusion algorithms [29], providing stable pose inputs for subsequent joint angle calculations.

Despite achieving promising results, this study has several limitations that warrant discussion.

First, the system is designed exclusively for offline post-hoc analysis. The current DTW computation requires approximately 2.3 seconds per trial, which is approximately 23 times greater than the <100 ms response time required for real-time gait correction or biofeedback applications. This is an intentional

design trade-off: decoupling data acquisition from computation achieves higher alignment accuracy without imposing embedded processing constraints. The offline paradigm is well-suited for clinical gait assessment, retrospective outcome monitoring, and longitudinal rehabilitation tracking. Future work will explore sliding-window DTW [15] implemented on embedded platforms such as ARM Cortex-M or NVIDIA Jetson Nano, targeting sub-100 ms latency for prospective rehabilitation feedback applications.

Second, the differential accuracy between hip and knee joints warrants a mechanistic discussion. The hip joint average RMSE of 4.1° is consistent with previously reported values for quaternion-based IMU systems [12], while the knee RMSE of 10.2° reflects the well-documented challenge of tracking joints with large flexion arcs using skin-mounted sensors. Three contributing factors are identified: (1) soft tissue artifact amplification — during stair negotiation, knee flexion of approximately 80°–110° causes substantial muscle bulk displacement beneath the elastic straps, violating the rigid-segment quaternion chain assumption [30]; (2) sensor-to-segment alignment sensitivity — the sagittal-plane extraction formula is sensitive to out-of-plane rotations, and the secondary valgus/varus and axial rotation of the knee during stair activities introduce cross-talk errors [21]; (3) functional calibration limitations — the N-pose static calibration does not account for dynamic misalignment that accumulates during loaded stair activities. Future work will investigate functional calibration protocols and constraint-based quaternion filtering to improve stair-scenario knee accuracy.

Third, the elastic strap fixation system provides insufficient constraint against soft tissue artifact (STA) during loaded stair activities, contributing to the observed RMSE elevation from 7.8° (flat walking) to 11.4° (stair negotiation) [30]. Two mitigation strategies are proposed: on the hardware side, replacing elastic straps with semi-rigid thermoplastic cuffs would reduce sensor-segment relative motion; on the algorithm side, an adaptive stance-phase correction module using heel contact events could re-anchor the quaternion chain to anatomically grounded reference frames between steps, suppressing drift accumulation without additional hardware.

Fourth, the participant cohort was limited to eight healthy young adults (aged 22–28 years), which restricts generalizability to broader populations, including individuals with pathological gait patterns such as post-stroke or Parkinson's disease, and elderly adults whose reduced walking speed may challenge the fixed 3 m/s² heel velocity threshold [2]. Additionally, the current system does not address the practical ease of sensor self-donning for home use. In a clinical setting, trained personnel assist with sensor placement; however, independent use by elderly individuals or patients with motor impairments — who must self-position five IMUs and perform the N-pose calibration — presents a usability challenge that has not been formally evaluated. Future studies should expand enrollment to include diverse clinical populations and conduct a standardized usability assessment to support translation to home-based rehabilitation monitoring.

Fifth, the single-master I2C bus architecture presents scalability constraints for whole-body kinematics capture. Transitioning to a BLE 5.0 wireless architecture with synchronized advertising intervals would be advisable for future expanded configurations.

Finally, the present system provides kinematic data only. Integrating pressure-sensing insoles to capture ground reaction forces (GRF) within an inverse dynamics framework would enable the estimation of net joint moments — relevant to osteoarthritis assessment, post-surgical rehabilitation monitoring, and fall risk stratification [19] — substantially expanding the system's clinical utility.

V. Conclusion

This study successfully evaluated the accuracy and reliability of a low-cost IMU-based system for measuring lower limb joint angles during flat walking, stair ascent, and stair descent. The findings demonstrate that the system provides precise and clinically relevant kinematic data, particularly for hip joint angles, while the DTW-based time alignment achieved a 29.1% reduction in average RMSE. Although knee joint accuracy was slightly lower — exceeding the 10° clinical threshold during stair negotiation — the system overall offers valuable insights into lower limb gait mechanics across multiple daily-life scenarios. Beyond kinematics, future integration of pressure-sensing insoles would enable ground reaction force measurement and inverse dynamics estimation of joint moments, substantially expanding the system's clinical utility for osteoarthritis assessment and rehabilitation monitoring. With its potential applications in clinical settings and community rehabilitation, further development in this area could lead to meaningful advancements in gait analysis and fall prevention strategies.

The findings underscore the promise of wearable inertial sensing technology in enhancing the objective assessment of human movement, paving the way for more accessible and data-driven rehabilitation techniques.

References

[1] Laidig D, Seel T. VQF: Highly accurate IMU orientation estimation with bias estimation and magnetic disturbance rejection. *Information Fusion*. 2023;91:187-204. doi:10.1016/j.inffus.2022.10.014

[2] Voisard C, Knobel SEA, Bisi MC, et al. Automatic gait events detection with inertial measurement units: Healthy and pathological gait evaluation in real-world environment. *Frontiers in Neurology*. 2024;14:1247532. doi:10.3389/fneur.2023.1247532

[3] Shah VR, Dixon PC. Gait speed and task specificity in predicting lower-limb kinematics: A deep learning approach using inertial sensors. *Mayo Clinic Proceedings: Digital Health*. 2024 (online). doi:10.1016/j.mcpdig.2024.11.005

[4] Shull PB, Jirattigalachote W, Hunt MA, et al. Quantified self and human movement: A review of the current state of wearable sensing and big data analyses of human gait. *Gait & Posture*. 2014;40(1):11-19. doi:10.1016/j.gaitpost.2014.03.193

[5] Chen D, Zhang Y, Zeng J. MagDot: Drift-free, wearable joint angle tracking at low cost. *Proceedings of the ACM on Interactive, Mobile, Wearable and Ubiquitous Technologies*. 2024;7(4):1-27. doi:10.1145/3631423

[6] Hafer JF, Freedman Silvernail J, Hillstrom HJ, Boyer KA. Challenges and opportunities for using wearable sensors to assess gait biomechanics in daily life. *Journal of Biomechanics*. 2023;149:111508. doi:10.1016/j.jbiomech.2023.111508

[7] García-de-Villa S, Jiménez-Martín A, Castillo JC. Inertial sensors for human motion analysis: A comprehensive review. *IEEE Transactions on*

Instrumentation and Measurement. 2023;72:1-21. doi:10.1109/TIM.2023.3264046

[8] Hafer JF, Boyer KA. Variability of segment coordination using a vector coding technique: Reliability analysis for treadmill walking and running. *Gait & Posture*. 2017;51:222-227. doi:10.1016/j.gaitpost.2016.11.004

[9] Seel T, Raisch J, Schauer T. IMU-based joint angle measurement for gait analysis. *Sensors*. 2014;14(4):6891-6909. doi:10.3390/s140406891

[10] Chen H, Schall MC Jr, Fethke NB. Drift-free joint angle calculation using inertial measurement units without magnetometers: An exploration of sensor fusion methods for the elbow and wrist. *Sensors*. 2023;23(16):7053. doi:10.3390/s23167053

[11] Cereatti A, Camomilla V, Vannozzi G, Cappozzo A. Propagation of the hip joint centre location error to the estimate of femur vs pelvis orientation using a constrained or an unconstrained approach. *Journal of Biomechanics*. 2017;62:140-147. doi:10.1016/j.jbiomech.2017.04.023

[12] Kobsar D, Charlton JM, Tse CTF, et al. Validity and reliability of wearable inertial sensors in healthy adult walking: A systematic review and meta-analysis. *Journal of NeuroEngineering and Rehabilitation*. 2020;17:62. doi:10.1186/s12984-020-00685-3

[13] Renggli D, Graf C, Tachatos N, et al. Wearable inertial measurement units for assessing gait in real-world environments. *Frontiers in Physiology*. 2020;11:90. doi:10.3389/fphys.2020.00090

[14] Zeng Z, Liu Y, Hu X, et al. Validity and reliability of inertial measurement units on lower extremity kinematics during running: A systematic review and meta-analysis. *Frontiers in Bioengineering and Biotechnology*. 2022;10:1005496. doi:10.3389/fbioe.2022.1005496

[15] Sakoe H, Chiba S. Dynamic programming algorithm optimization for spoken word recognition. *IEEE Transactions on Acoustics, Speech, and Signal Processing*. 1978;26(1):43-49. doi:10.1109/TASSP.1978.1163055

[16] Manupibul U, Tanthuwapathama R, Jarumethitanont W, et al. Integration of force and IMU sensors for developing low-cost portable gait measurement system in lower extremities. *Scientific Reports*. 2023;13:11914. doi:10.1038/s41598-023-37761-2

[17] Tang L, Li Y, Wang H, et al. IMU-based real-time estimation of gait phase using multi-sensor fusion. *Sensors*. 2024;24(8):2390. doi:10.3390/s24082390

[18] Wu B, Zhang X, Chen Y, et al. A novel personalized strategy for hip joint flexion angle prediction based on a NARX neural network. *Biosensors*. 2024;14(9):418. doi:10.3390/bios14090418

[19] Inai T, Kobayashi Y, Furukawa M, et al. Errors in estimating lower-limb joint angles and moments during gait using lower-limb inertial measurement units and one inertial measurement unit on the waist: A simulation study. *Sensors*. 2024;24(16):5320. doi:10.3390/s24165320

[20] Shiao Y, Zheng W, Lin C, et al. Three-dimensional human posture recognition by multiangular camera acquisition and deep learning recognition. *Sensors*. 2024;24(13):4306. doi:10.3390/s24134306

[21] Potter MV, Ojeda LV, Perkins NC, et al. Simulating effects of sensor-to-segment alignment errors on lower-limb joint angle estimation during running. *Sports Engineering*. 2025;28:5. doi:10.1007/s12283-024-00483-3

[22] Bonfiglio A, Lulic-Kuryllo T, Hoitz F, et al. Effects of different inertial measurement unit sensor-to-segment alignments on gait performance measures. *Journal of Applied Biomechanics*. 2024;40(3):201-212. doi:10.1123/jab.2023-0276

[23] Cisnal A, Pérez-Turiel J, Fraile JC, et al. Dynamic time warping-based gait recognition using inertial sensors. Gait & Posture. 2023;102:56-63. doi:10.1016/j.gaitpost.2023.03.012

[24] Wang X, Kyrarini M, Ristić-Durrant D, et al. Monitoring of gait performance using dynamic time warping on IMU-sensor data. Proc IEEE Int Symp Med Meas Appl (MeMeA). 2016:1-5.

[25] Tao W, Liu T, Zheng R, Feng H. Gait analysis using wearable sensors. Sensors. 2012;12(2):2255-2283. doi:10.3390/s120202255

[26] Zhang Y, Li X, Chen Y, et al. A low-cost wearable system for joint angle measurement using IMU and flexible sensor fusion. IEEE Sensors J. 2023;23(2):1589-1598. doi:10.1109/JSEN.2022.3219187

[27] Steinmetzer T, Bonninger I, Priwitzer B, et al. Analyzing gait symmetry with automatically synchronized wearable sensors in daily life. Microprocessors and Microsystems. 2020;77:103118. doi:10.1016/j.micpro.2020.103118

[28] Madgwick SOH, Harrison AJL, Vaidyanathan R. Estimation of IMU and MARG orientation using a gradient descent algorithm. IEEE International Conference on Rehabilitation Robotics. 2011:1-7. doi:10.1109/ICORR.2011.5975346

[29] Caruso M, Sabatini AM, Knaflitz M, et al. Analysis of the accuracy of ten algorithms for orientation estimation using inertial and magnetic sensing under optimal conditions: One size does not fit all. Sensors. 2021;21(7):2543. doi:10.3390/s21072543

[30] Peters A, Galna B, Sangeux M, et al. Quantification of soft tissue artifact in lower limb human motion analysis: A systematic review. Gait & Posture. 2010;31(1):1-8. doi:10.1016/j.gaitpost.2009.09.004